BULLETIN OF THE CHEMICAL SOCIETY OF JAPAN VOL. 43 3780—3789 (1970)

Far Infrared Transmission Spectra and Lattice Vibrations of $RbNiF_3$ and $CsNiF_3$

Kay KOHN*1 and Ichiro NAKAGAWA

Department of Chemistry, Faculty of Science, The University of Tokyo, Hongo, Tokyo

(Received July 21, 1970)

The infrared absorption spectra of $RbNiF_3$ and $CsNiF_3$, both with a perovskite-like structure, have been measured in the region 500—50 cm^{-1} at room temperature and at liquid nitrogen temperature. The observed bands can be classified into three groups, corresponding to the three absorption bands in perovskite. These bands can reasonably be assigned on the basis of the crystal symmetry of the investigated compounds. A normal coordinate analysis of a crystal as a whole has been performed, where the interatomic force constants between the atom pairs within a distance of 3.5 Å are taken into account. It was shown that the normal coordinate treatment of the optically-active vibrations on the basis of a molecular dynamics model is useful for the interpretation of the lattice vibrations in these fluorides. The effects of the structural differences of the lattice vibrations are discussed.

In recent years several investigations of lattice vibrations in perovskite-type fluorides AMF_3 have been made, and the nature of the interatomic forces in these compounds is coming to be clear.[1–5] The observed infrared spectra were well interpreted on the basis of a valence force type potential for MF_6-octahedron and a central force type potential for the other atom pairs, A-F, F-F, and M-A.[5] This means that some covalent character is included in the M-F bond, even in the "ionic" crystal AMF_3.

Various compounds with the composition AMX_3, which have a crystal structure closely related to the perovskite structure, have been discovered, and the stability relations among these structures have been discussed.[6,7] All these compounds are com-

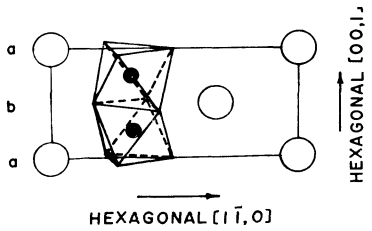

(a)

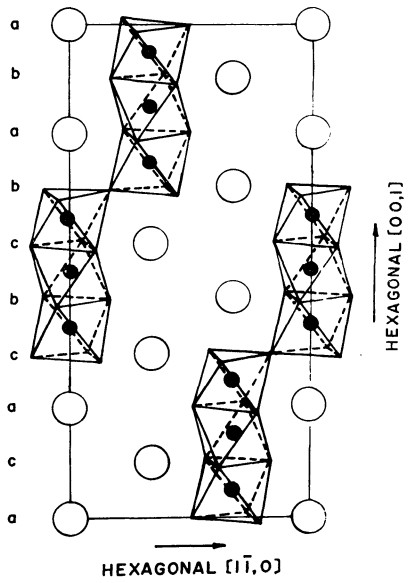

(b)

*1 On leave from the Department of Physics, School of Science and Engineering, Waseda University, Nishi-okubo, Tokyo.

1) G. R. Hunt, C. H. Perry and J. Furguson, *Phys. Rev.*, **134**, A688 (1964).

2) C. H. Perry, *Japanese J. Appl. Phys., Suppl.* 1, **4**, 564 (1965).

3) A. S. Barker, Jr., *Phys. Rev.*, **136**, A1290 (1964).

4) M. Balkanski, P. Moch and G. Parisot, *J. Chem. Phys.*, **44**, 940 (1966).

5) I. Nakagawa, A. Tsuchida and T. Shimanouchi, *ibid.*, **47**, 982 (1967).

6) Y. Syono, S. Akimoto and K. Kohn, *J. Phys. Soc. Jap.*, **26**, 993 (1969).

7) J. M. Longo and J. A. Kafalas, *Solid State Chem.*, **1**, 103 (1969).

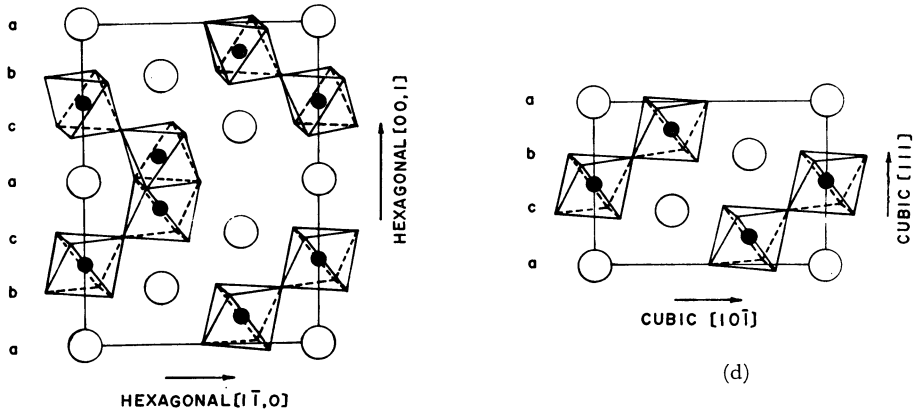

Fig. 1. Crystal structures of $RbNiF_3$ and $CsNiF_3$. All Ni (full circle) and Rb or Cs (open circle) ions on the hexagonal (1.1, 0) plane are illustrated. F ions are located on the octahedra around Ni ions. (a) $CsNiF_3$ 2L, (b) $CsNiF_3$ 9L, (c) $RbNiF_3$ 6L, (d) $RbNiF_3$ cubic.

posed of closely-packed layer lattice of larger cations, A, and anions, X, while smaller cations, M, are located at the octahedral interstices of the AX_3 lattice. The only difference between the several structures is in the stacking order of the closely-packed layers. If we denote the three different phases of such layers in a closely-packed structure as *a*, *b*, and *c*, an ordinary perovskite may be expressed as *abcabc*. The structures with the stacking sequences *ab* (2-layer type: 2L), *abcacb* (6-layer type: 6L), and *ababcbcac* (9-layer type: 9L) appear in fluorides, as is shown in Fig. 1.

The purpose of the present study is to investigate how these structural differences are reflected in the infrared spectra and to clarify the lattice vibrations in these "perovskite-like" compounds. Our aims are to establish the actual forms of vibrations, to test the validity of the pictures used for perovskites in a previous work by one of the present authors (I. N.) on these compounds, and, further, to establish the interrelations between the nature of the bonds and the stabilities of the various structures. For this purpose we have chosen to study two fluorides, $RbNiF_3$ and $CsNiF_3$. $RbNiF_3$ has a 6-layer structure (hexagonal $BaTiO_3$ structure) at ordinary pressure, and it is transformed into a cubic perovskite structure at 10 kbar.[6] $CsNiF_3$ has 2-layer structure at ordinary pressure, and it is transformed into a 9-layer structure at a few kbar.[8,9] Thus, we can compare different structures with the same composition.

We measured the far infrared transmission spectra at room temperature and at liquid nitrogen temperature. We also calculated the lattice vibrations on the same assumptions regarding interatomic forces as in the previous paper. The results show that the picture applied to perovskites is also valid in "perovskite-like" fluorides. The potential constants, which give calculated frequencies in good agreement with the observed, were also determined.

Experimental

Polycrystalline $RbNiF_3$ 6L and $CsNiF_3$ 2L were prepared from an intimate mixture of RbF and NiF_2 or CsF and NiF_2 by reaction at an elevated temperature. The reaction was made in a sealed-off platinum ampoule in order to prevent oxidation and evaporation. The high pressure phases, $RbNiF_3$ cubic and $CsNiF_3$ 9L, were supplied by Dr. Y. Syono of the Institute for Solid State Physics of the University of Tokyo. They were prepared from the corresponding low pressure phases using a tetrahedral anvil type, high pressure apparatus. These samples were dispersed in polyethylene sheets for use in the measurements.

A Hitachi FIS-I vacuum infrared spectrometer (500—50 cm^{-1}) was used. In the low-temperature measurements, samples were placed in direct contact with the metal conductor in the cryostat, and spectral measurements were made according to the procedure described in a previous paper.[5] The observed spectra are reproduced in Fig. 2.

Spectral measurements are limited to the transmittance, and throughout this study we regard the absorption frequencies obtained from the powder samples as ν's (resonance frequencies or minimum transmission frequencies as a thickness $d \to 0$). We checked the difference between the resonance frequencies obtained from the reflection data of a single crystal and those from the transmission data of a powder sample for a closely-related compound, MgF_2, for which both crystal and powder samples are available. This difference was found to be less than 5%, as will be shown in Appendix1.

8) Y. Syono, S. Akimoto and K. Kohn, presented at Colloque International du C.N.R.S. sur les Propriétés Physiques des Solides sous Pression (Grenoble, Sept. 1969).

9) J. M. Longo and J. A. Kafalas, *J. Appl. Phys.*, **40**, 1601 (1969).

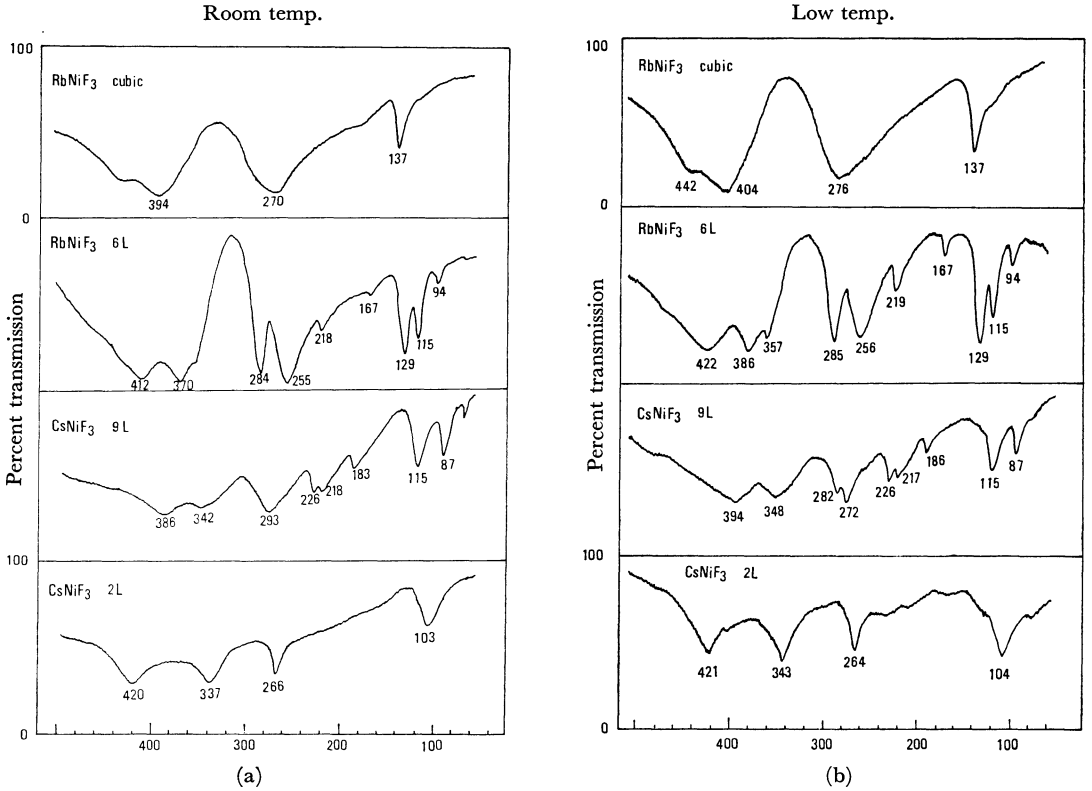

Fig. 2. Infrared absorption spectra of $RbNiF_3$ and $CsNiF_3$. Powdered samples dispersed in polyethylene sheets (*ca.* 1 mg/cm²). (a) spectra of room temperature, (b) spectra of liquid nitrogen temperature.

Observed Spectra

The observed spectrum of $RbNiF_3$ cubic is similar to that of the isomorphous compound $KNiF_3$. It consists of three absorption bands, around 390 cm^{-1}, 270 cm^{-1}, and 140 cm^{-1}. It is clear that they correspond to the Ni-F stretching, F-Ni-F bending, and A-F stretching vibrations respectively. Many more bands appeared in the spectra of $RbNiF_3$ 6L and $CsNiF_3$ 9L. They can also be classified into three groups, the bands in the 350—420 cm^{-1} range, those in the 200—300 cm^{-1} range, and those below 200 cm^{-1}. It can easily be understood that these bands arise from the splitting of the above three bands in more complicated structures. The spectrum of $CsNiF_3$ 2L consists of four bands. The two bands at lower frequencies are considered to arise from the F-Ni-F bending and Cs-F stretching vibrations. However, the two at 420 cm^{-1} and 340 cm^{-1} are either too high or too low to be simply compared with the corresponding band of cubic perovskite.

With a lowering of the temperature almost all the bands become sharp, and a few split into several components. At the same time, they shift to higher frequencies. Among them, the bands around 400 cm^{-1} show the most remarkable shift.

Lattice Vibrations of "Perovskite-like" Fluorides

The crystal structures of $RbNiF_3$ 6L, $RbNiF_3$ cubic, $CsNiF_3$ 2L,[10] and $CsNiF_3$ 9L (Fig. 1) belong to the space groups D^4_{6h}—$P6_3/mmc$, $O^1{}_h$—$Pm3m$, D^4_{6h}—$P6_3/mmc$, and D^5_{3d}—$R\bar{3}m$, and the Bravais primitive cells of these compounds consist of 6, 1, 2, and 3 formula units respectively. The crystallographic data relevant to later discussions are summarized in Table 1. The numbers of optically-active lattice vibrational modes in the different species were determined by factor-group analysis.[11] The results are shown in Table 2.

The optically-active vibrational frequencies and the corresponding vibrational modes were calculated according to the method of Shimanouchi, Tsuboi, and Miyazawa.[12] First, we took a potential function:

$$U = \frac{1}{2}\sum_{i,j} K_i(\Delta r_{\text{Ni-F}}{}^i{}_j)^2 + \frac{1}{2}\sum_{i,j} H_i(\Delta\alpha_{\text{F-Ni-F}}{}^i{}_j)^2 + \frac{1}{2}\sum_{i,j} F_i(\Delta q_{\text{F-F}}{}^i{}_j)^2 + \frac{1}{2}\sum_{i,j} f_i(\Delta q_{\text{A-F}}{}^i{}_j)^2$$

10) D. Babel, *Z. Naturforsch.*, **20a**, 165 (1965).

11) See, for example, S. Bhagavantam and T. Venkatarayudu, "Theory of Groups and Its Applications to Physical Problems," (2nd ed.), Andhra Univ., Waltair, 1951, p. 127.

12) T. Shimanouchi, M. Tsuboi and T. Miyazawa, *J. Chem. Phys.*, **35**, 1597 (1961).

TABLE 1. CRYSTAL DATA OF $RbNiF_3$ AND $CsNiF_3$

Compound	Structure Space group	Lattice Parameters	Ionic positions
$RbNiF_3$ 6L	6 layer $D_{6h}^4-P6_3/mmc$	$a=5.847$Å $c=14.319$Å $Z=6$	Rb 1 in $2(b)$ Rb 2 in $4(f)$ $(z=0.0986)$[a] Ni 1 in $2(a)$ Ni 2 in $4(f)$ $(z=0.8498)$[a] F 1 in $6(h)$ $(x=0.522)$[a] F 2 in $12(k)$ $(x=0.835, z=0.078)$[a]
$RbNiF_3$ cubic	perovskite O_h^1-Pm3m	$a=4.0769$Å $Z=1$	Rb in $1(a)$ Ni in $1(b)$ F in $3(c)$
$CsNiF_3$ 2L	2 layer $D_{6h}^4-P6_3/mmc$	$a=6.255$Å $c=5.237$Å $Z=2$	Cs in $2(c)$ Ni in $2(a)$ F in $6(h)$ $x=-0.1431$[b]
$CsNiF_3$ 9L	9 layer $D_{3d}^5-R\bar{3}m$	$a=6.146$Å $c=22.300$Å $Z=9$ (hexagonal cell)	Cs 1 in $3(a)$ Cs 2 in $6(c)$ $(z=0.2181)$[c] Ni 1 in $3(b)$ Ni 2 in $6(c)$ $(z=0.3819)$[c] F 1 in $9(e)$ F 2 in $18(h)$ $(x=0.156, z=0.558)$[c]

a) see Ref. 13) for $CsMnF_3$
b) see Ref. 10)
c) see Ref. 14) for $BaRuO_3$

TABLE 2. RESULT OF FACTOR GROUP ANALYSIS FOR OPTICALLY ACTIVE LATTICE VIBRATIONS OF $RbNiF_3$ AND $CsNiF_3$

Space group	Compounds	Number of modes in each species
$D_{6h}^4-P6_3/mmc$	$RbNiF_3$ 6L	$5A_{1g}+1A_{1u}+2A_{2g}+6A_{2u}$ $+6B_{1g}+2B_{1u}+1B_{2g}$ $+6B_{2u}+8E_{1g}+8E_{1u}$ $+6E_{2g}+7E_{2u}$ IR active: A_{2u} and E_{1u} (acoustical modes: $1A_{2u}$ $+1E_u$)
O_h^1-Pm3m	$RbNiF_3$ cubic	$3F_{1u}+1F_{2u}$ IR active: F_{1u} (acoustical modes: $1F_{1u}$)
$D_{6h}^4-P6_3/mmc$	$CsNiF_3$ 2L	$1A_{1g}+1A_{2g}+2A_{2u}+2B_{1g}$ $+1B_{1u}+2B_{2u}+3E_{1g}$ $+3E_{1u}+1E_{2g}+2E_{2u}$ IR active: A_{2u} and E_{1u} (acoustical modes: $1A_{2u}$ $+1E_{1u}$)
D_{3d}^5-R3m	$CsNiF_3$ 9L	$4A_{1g}+2A_{1u}+1A_{2g}+7A_{2u}$ $+5E_g+9E_u$ IR active: A_{2u} and E_u (acoustical modes: $1A_{2u}$ $+1E_u$)

where K_i's and H_i's denote the Ni-F bond-stretching and F-Ni-F angle-bending force constants. The f_i's and F_i's represent the interactions between the A cations (Rb^+ or Cs^+) and the F^- ions, and those between F^- ions, respectively. The sum was taken over all kinds of internal coordinates, i, and all the internal coordinates, j, for each kind of i in a Bravais primitive cell. These potential is a generalization of the potential function described in the previous paper. That is, we assumed a valence force type potential for the NiF_6-octahedron, and a central force type potential for all the atom pairs, for which the nonbonded repulsions or the ionic interactions are expected to be considerable. In the present case, all the interactions between the atom pairs within a distance of 3.5 Å were taken into account.

The internal coordinates, in which the potential function is expressed, are transformed into Cartesian diplacement coordinates, and the potential function is expressed in terms of Cartesian displacement coordinates. The optically-active $\boldsymbol{F}$-matrix (potential energy matrix), $\boldsymbol{F}_{\mathrm{op}}$, in terms of the optically-active Cartesian displacement coordinates, is set up; the secular equation,

$$|\boldsymbol{M}^{-1}\boldsymbol{F}_{\boldsymbol{x}\,\mathrm{op}}-\boldsymbol{E}\lambda|=0$$

where $\boldsymbol{M}$ is a diagonal mass matrix and $\boldsymbol{E}$ is an unit matrix, gives the eigenvalues and eigenvectors which correspond to the frequencies and the vibrational modes. The normal modes are described on the basis of the Cartesian symmetry coordinates listed in Appendix 2.

In the course of the calculation, the values of the atomic positions and interatomic distances were needed. They were calculated using the lattice parameters given in Table 1. Since precise crystal data were lacking for $RbNiF_3$ 6L and $CsNiF_3$ 9L, we used some parameter values of isomorphous

13) A. Zalkin, K. Lee and D. H. Templeton, *J. Chem. Phys.*, **37**, 697 (1962).
14) P. C. Donohue, L. Katz and R. Ward, *Inorg. Chem.*, **4**, 306 (1965).

compounds, $CsMnF_3$ (6L type) and $BaRuO_3$ (9L type). They are given in parentheses in Table 1. This is justified since the corresponding parameter values in $CsMnF_3$[13] and hexagonal $BaTiO_3$,[15] both of which have a 6L-type structure, are quite the same.

TABLE 3. CALCULATED AND OBSERVED FREQUENCIES OF INFRARED ACTIVE VIBRATIONS IN $RbNiF_3$ AND $CsNiF_3$

$RbNiF_3$ 6L			$RbNiF_3$ cubic	
Calcd. (A_{2u}) cm^{-1}	Calcd. (E_{1u}) cm^{-1}	Obsd. cm^{-1}	Calcd. (F_{1u}) cm^{-1}	Obsd. cm^{-1}
411	411	412	394	394
352		370	273	270
	325	354	129	137
	286	284		
243	253			
	204	218		
183	178	167		
106	112	129 115		
85	82	94		

$CsNiF_3$ 2L			$CsNiF_3$ 9L		
Calcd. (A_{2u}) cm^{-1}	Calcd. (E_{1u}) cm^{-1}	Obsd. cm^{-1}	Calcd. (A_{2u}) cm^{-1}	Calcd. (E_u) cm^{-1}	Obsd. cm^{-1}
		420	370	366	386
350	348	337	347	326	342
	231	266	317		
	81	103			
55			265	289 276	273 (doublet)
				250	226
				205	218
			171		183
			107	129 104	115
			71	69	87

The numerical calculations were carried out with a HITAC 5020E computer at the Computation Center of the University of Tokyo. Programs, AXSM and CART, set up in our laboratory were used.[16] The calculated frequencies of optically-active vibrations are listed in Table 3, together with the observed values. The values of the force constants are given in Table 4. All the force constants were determined in a consistent way, in the sense that the relation between the interatomic distances and force constants was taken as universal for all the fluorides in the present study as well as for perovskite $KNiF_3$ in the previous paper. The following points should be made:

1) The force constants K_i's and F_i's are assumed to be functions of the interatomic distances r_{Ni-F} and r_{F-F}, respectively, regardless of the composition or structure of the compound (see Figs. 3 and 4).

2) The force constants H_i's are taken to have a constant value of 0.30 mdyn·Å in all cases.

3) The force constants f_i's are assumed to be a linear function of the ratio of the actual bond length, r_{A-F}, to the sum of the ionic radii, $r_{A^+}+r_{F^-}$ (see Fig. 5).

TABLE 4(a). FORCE CONSTANTS K_i USED IN THE CALCULATION

Compound	Kind of bond	Bond length (Å)	K_i (mdyn/Å)
$RbNiF_3$ 6L	Ni 2-F 2	1.99	0.70
$RbNiF_3$ 6L	Ni 1-F 2	2.01	0.64
$CsNiF_3$ 2L	Ni 1-F 1	2.03	0.60
$RbNiF_3$ cubic	Ni 1-F 1	2.04	0.58
$RbNiF_3$ 6L	Ni 2-F 1	2.05	0.57
$CsNiF_3$ 9L	Ni 2-F 1	2.09	0.55
$CsNiF_3$ 9L	Ni 1-F 2	2.10	0.54
$CsNiF_3$ 9L	Ni 2-F 2	2.13	0.53

TABLE 4(b). FORCE CONSTANTS f_i USED IN THE CALCULATION

Compound	Kind of bond	Bond length (Å)	f_i (mdyn/Å)
$RbNiF_3$ cubic	Rb 1-F 1	2.88	0.14
$RbNiF_3$ 6L	Rb 2-F 1	2.89	0.14
$RbNiF_3$ 6L	Rb 1-F 1	2.93	0.12
$RbNiF_3$ 6L	Rb 2-F 2	2.94	0.12
$RbNiF_3$ 6L	Rb 1-F 2	2.98	0.10
$RbNiF_3$ 6L	Rb 2-F 2	3.05	0.07
$CsNiF_3$ 9L	Cs 1 -F 1	3.07	0.13
$CsNiF_3$ 9L	Cs 1 -F 2	3.07	0.13
$CsNiF_3$ 9L	Cs 2 -F 2	3.08	0.13
$CsNiF_3$ 9L	Cs 2 -F 2	3.08	0.13
$CsNiF_3$ 9L	Cs 2 -F 1	3.12	0.11
$CsNiF_3$ 2L	Cs 1 -F 1	3.14	0.09
$CsNiF_3$ 2L	Cs 1 -F 1	3.33	0.03

Discussion of Results

The spectrum of $RbNiF_3$ cubic reveals a typical feature characteristic of a regular cubic perovskite structure. The three absorption bands observed correspond to the Ni-F stretching, F-Ni-F angle

15) P. C. Burbank and H. T. Evans, Jr., *Acta Crystallogr.*, **1**, 330 (1948).

16) T. Shimanouchi, "Computer Programs for Normal Coordinate Treatment of Polyatomic Molecules," The University of Tokyo, July 1968.

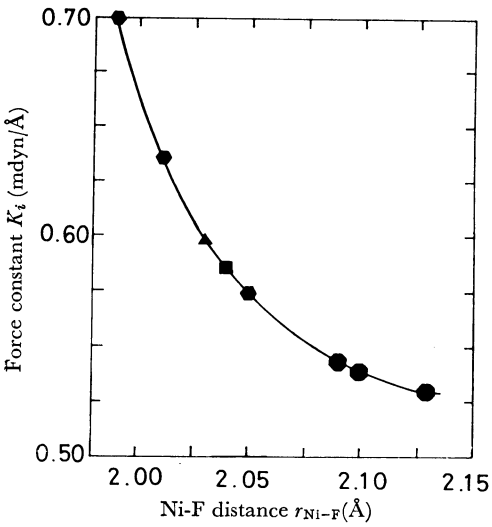

Fig. 3. Dependence of force constants K_i's used in the calculation on interatomic distance r_{Ni-F}. ⬢ $RbNiF_3$ 6L, ■ $RbNiF_3$ cubic, ▲ $CsNiF_3$ 2L ● $CsNiF_3$ 9L

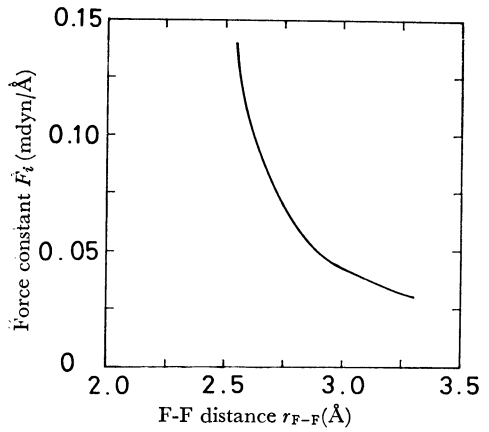

Fig. 4. Dependence of force constants F_i's used in the calculation on interatomic distance r_{F-F}.

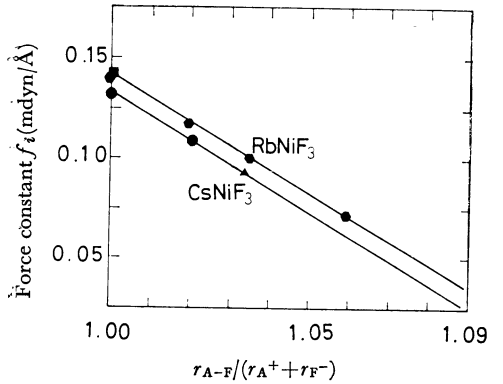

Fig. 5. Dependence of force constants f_i's used in the calculation on the ratio of the actual bond length r_{A-F} to the sum of ionic radii $r_A + r_F$.

bending, and Rb-F stretching modes respectively, all of which belong to the F_{1u} species. In contrast with this simple spectrum, those of $RbNiF_3$ 6L and $CsNiF_3$ 9L are much more complicated. However, they can be explained if we consider that a single band in perovskite splits into several components in more complicated structures. This situation may be clearly seen in the form of the calculated normal modes of vibrations. In Fig.6(a) we show the atomic displacements for the normal modes of the lattice vibrations of $RbNiF_3$ 6L as an example. This is based on the transformation matrix, $\boldsymbol{L}_x$, between the Cartesian coordinates, $\boldsymbol{X}$ and the normal coordinates $\boldsymbol{Q}$, defined as $\boldsymbol{X}=\boldsymbol{L}_x\boldsymbol{Q}$, $\boldsymbol{M}^{-1}\boldsymbol{F}_x\boldsymbol{L}_x=\boldsymbol{L}_x\boldsymbol{\Lambda}$. Here we will examine how the above splittings come about in the Ni-F stretching modes in $RbNiF_3$ 6L. In this phase Ni ions are still surrounded by six F^- ions, as in perovskite-type $RbNiF_3$. However, we can expect that a single band in $RbNiF_3$ cubic will split, since:

1) there are two different sites, (*a*) and (*f*), for Ni ions and the vibrational modes of these NiF_6-octahedra couple together to give two different frequencies;

2) these NiF_6-octahedra are not regular, unlike in perovskite, but are somewhat distorted in different ways (Table 5), and

Table 5. Distortion of NiF_6-octahedra in $RbNiF_3$ and $CsNiF_3$

Compound	Central Ni ion[a)]	Ni-F bond length (Å)	F-Ni-F bond angle
$RbNiF_3$ 6L	Ni 1	2.01	92.1°
	Ni 2	1.99	95.5°
		2.05	76.6°
$RbNiF_3$ cubic	Ni 1	2.04	90°
$CsNiF_3$ 2L	Ni 1	2.10	82.8°
$CsNiF_3$ 9L	Ni 1	2.10	86.2°
	Ni 2	2.08	84.7°
		2.13	95.3°

a) See Table 1.

3) some of the freedom of motion of the F^- ions is inhibited by the symmetry in infrared active vibrations, and the form of the vibrational modes of a single octahedron undergoes some change. It may clearly be seen in Fig. 6 that a simple vibrational mode in perovskite (Fig. 6b) is modified, and that some modes have a feature of the partially angle-bending type. This tendency is essentially the same for all the compounds studied here.

The reasonable agreement between the calculated and the observed frequencies suggests that our model is still applicable to these fluorides. However, we must remark on several points in this connection. First, there are some differences between the values of the force constants K_i's used in this paper and those determined for some perovskite-type fluorides

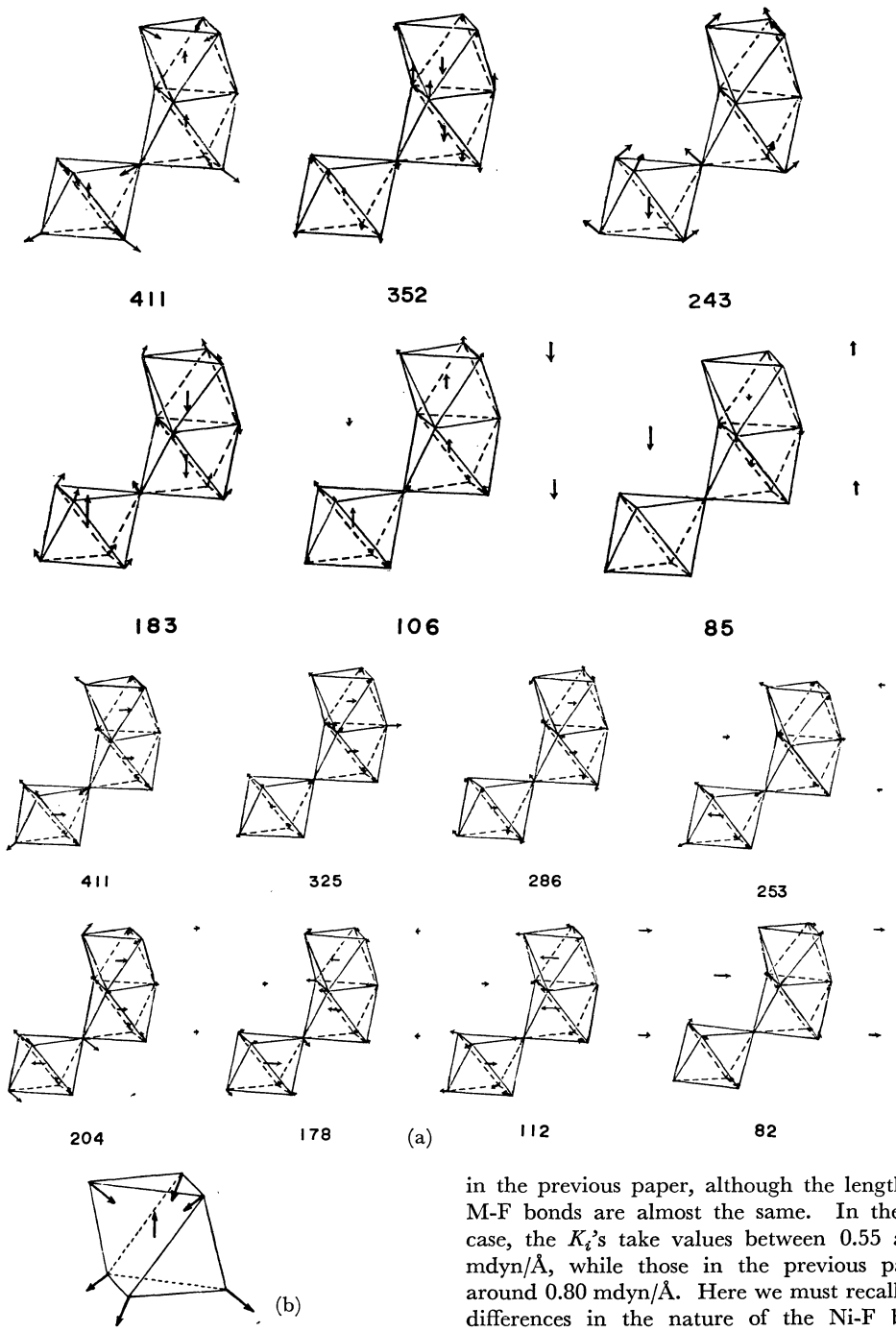

Fig. 6. (a) Displacements of ions for the lattice vibrational modes in $RbNiF_3$ 6L. Only a half of Bravais primitive cell is shown, since the displacements of other ions can be derived by considering inversion symmetry of the modes. The vibrational modes of A_{2u} and E_{1u} species are illustrated in upper and lower halves, respectively. (b) Displacements of ions in MF_6-octahedron for the Ni-F stretching vibrational mode in perovskite type fluoride.

in the previous paper, although the lengths of the M-F bonds are almost the same. In the present case, the K_t's take values between 0.55 and 0.70 mdyn/Å, while those in the previous paper are around 0.80 mdyn/Å. Here we must recall possible differences in the nature of the Ni-F bonds in these two cases. Some of the compounds in this study have a high pressure form, and the atoms are, so to speak, "squeezed together" in them. This will certainly cause a deviation of the force constants from their values in ordinary structures. In addition, there is some change in the covalent character in Ni-F bonds, as is suggested by the distortions of the NiF_6-octahedra. The distortion of NiF_6-octahedra are listed in Table 5. The

covalent character differs from one type of octahedron to another. Such factors are wholly neglected in our calculation, where the K_i's are taken as a function of the bond length only, and where the H_i's are assumed to be constant regardless of the actual bond angles. For instance, in $RbNiF_3$ 6L, the octahedron around the *f*-site Ni ions is much distorted. This suggests some modifications in some force constants, which results in the improvement in some of the calculated frequencies (352, 325, 286, 183, and 178 cm^{-1}). At present, however, we have no sound theoretical ground or empirical information sufficient to guide our estimation of the force constants in such cases. Thus, our simple model serves only as a useful starting point. The force constants, f_i's and F_i's, between nonbonded ions are more satisfactorily used.

As for $CsNiF_3$ 2L, we have some trouble in explaining the Ni-F stretching vibrations, since the calculated frequencies of the A_{2u} and E_{1u} species for this mode are almost the same, while we have two observed bands around 420 cm^{-1} and 340 cm^{-1}. An experimental check for isomorphous compounds is needed. A study about such compounds containing oxides and chlorides is now in progress.

The authors wish to express their thanks to Professor T. Shimanouchi of the University of Tokyo for his kind guidance and valuable discussions. Thanks are also due to Professor S. Akimoto and Dr Y. Syono of the Institute for Solid State Physics of the University of Tokyo for kindly supplying the samples of high pressure phases of $RbNiF_3$ and $CsNiF_3$.

Note Added in Proof.

Recently Dr D. Babel and Dr J. M. Longo have kindly informed us about their crystal data of $RbNiF_3$ 6-layer type (D. Babel: *Z. Anorg. Allgem. Chem.*, **369**, 117 (1969), R. J. Arnott and J. M. Longo: to be published in *J. Solid State Chem.*, **2**, (1970)). Their parameter values of ion sites are very close to those assumed in this paper.

Appendix 1. *Comparison of the Transmission Spectrum of Powdered Samples with the Reflection Spectrum of Single Crystals.*

The results of MgF_2 (uniaxial crystal: D_{4h}^{14}-*Pnnm*) are given in Fig. 7.

A transmission measurement of a MgF_2 powdered sample dispersed in a polyethylene sheet (*ca.* 1 mg/cm^2) was made by using a HITACHI EPI-L spectometer. A reflection measurement of the MgF_2 single crystal was made near a normal incidence on the *c*-plane, using HITACHI EPI-L and FIS-21 spectrometers with reflectance attachments. The optical constants were derived from the measured reflectivity, using the Kramers-Kronig relation.

The reflection spectrum and the real and imaginary parts of the infrared dielectric constant (ε' and ε'') are given in Fig. 7, where they are also compared with the transmission spectrum.

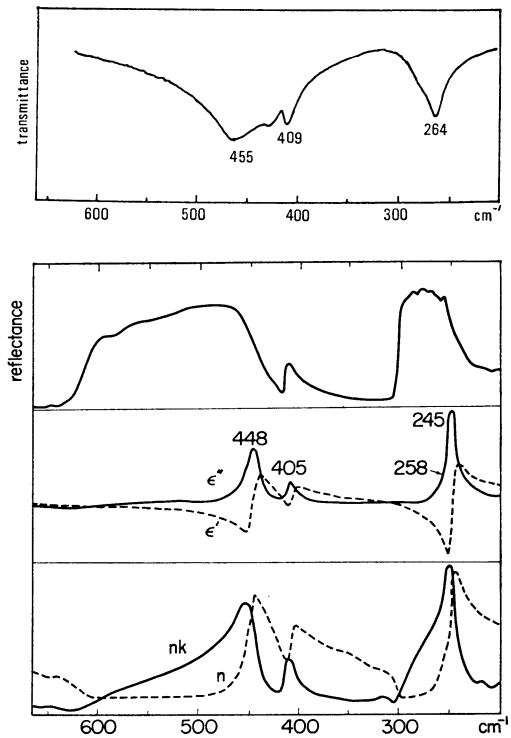

Fig. 7. Comparison of the transmission spectrum of powdered sample with the reflection spectrum of single crystal for MgF_2.

Appendix 2. *Cartesian Symmetry Coordinates of Infrared Active Vibrational Modes in "Perovskite-like" Compounds.*

The Cartesian symmetry coordinates of optically active vibrational modes in 2L, 6L, and 9L structures have been determined. The expressions for the infrared active vibrational modes are as follows:

1) $RbNiF_3$6L: Ions with the Cartesian coordinates given in the parenthesis are indexed as follows:

1 Ni 1; (0, 0, 0),
2 Ni 1; (0, 0, $c/2$),
3 Ni 2; ($-a/\sqrt{3}$, 0, w_{1c}),
4 Ni 2; ($-a/\sqrt{3}$, 0, $\overline{1/2-w_{1c}}$),
5 Ni 2; ($a/\sqrt{3}$, 0, $-w_{1c}$),
6 Ni 2; ($a/\sqrt{3}$, 0, $\overline{-1/2+w_{1c}}$),
7 F 1; ($(\sqrt{3}/2)u_{4a}$, $(-3/2)u_{4a}$, $c/4$),
8 F 1; ($-\sqrt{3}\,u_{4a}$, 0, $c/4$),
9 F 1; ($(\sqrt{3}/2)u_{4a}$, $(3/2)u_{4a}$, $c/4$),
10 F 1; ($\sqrt{3}\,u_{4a}$, 0, $-c/4$),
11 F 1; ($(-\sqrt{3}/2)u_{4a}$, $(3/2)u_{4a}$, $-c/4$),
12 F 1; ($(-\sqrt{3}/2)u_{4a}$, $(-3/2)u_{4a}$, $-c/4$),
13 F 2; ($-\sqrt{3}\,u_{2a}$, 0, w_{2c}),
14 F 2; ($(\sqrt{3}/2)u_{2a}$, $(-3/2)u_{2a}$, w_{2c}),
15 F 2; ($(\sqrt{3}/2)u_{2a}$, $(3/2)u_{2a}$, w_{2c}),
16 F 2; ($-\sqrt{3}\,u_{2a}$, 0, $\overline{1/2-w_{2c}}$),
17 F 2; ($(\sqrt{3}/2)u_{2a}$, $(-3/2)u_{2a}$, $\overline{1/2-w_{2c}}$),

18 F 2; $((\sqrt{3}/2)u_{2}a, (3/2)u_{2}a, \overline{1/2-w_{2}c})$,
19 F 2; $(\sqrt{3}u_{2}a, 0, -w_{2}c)$,
20 F 2; $((-\sqrt{3}/2)u_{2}a, (3/2)u_{2}a, -w_{2}c)$,
21 F 2; $((-\sqrt{3}/2)u_{2}a, (-3/2)u_{2}a, -w_{2}c)$,
22 F 2; $(\sqrt{3}u_{2}a, 0, \overline{-1/2+w_{2}c})$,
23 F 2; $((-\sqrt{3}/2)u_{2}a, (3/2)u_{2}a, \overline{-1/2+w_{2}c})$,
24 F 2; $((-\sqrt{3}/2)u_{2}a, (-3/2)u_{2}a, \overline{-1/2+w_{2}c})$,
25 Rb 1; $(0, 0, c/4)$,
26 Rb 1; $(0, 0, -c/4)$,
27 Rb 2; $(a/\sqrt{3}, 0, w_{3}c)$,
28 Rb 2; $(a/\sqrt{3}, 0, \overline{1/2-w_{3}c})$,
29 Rb 2; $(-a/\sqrt{3}, 0, -w_{3}c)$,
30 Rb 2; $(-a/\sqrt{3}, 0, \overline{-1/2+w_{3}c})$,

where u_i's and w_i's are parameter values (see Table 1). Then the Cartesian symmetry coordinates of A_{2u} and E_{1u} species are as follows.

(A_{2u})

Ni 1: $s_1=(1/\sqrt{2})\Delta(z_1+z_2)$,
Ni 2: $s_2=(1/\sqrt{4})\Delta(z_3+z_4+z_5+z_6)$,
Rb 1: $s_3=(1/\sqrt{2})\Delta(z_{25}+z_{26})$,
Rb 2: $s_4=(1/\sqrt{4})\Delta(z_{27}+z_{28}+z_{29}+z_{30})$,
F 1: $s_5=(1/\sqrt{6})\Delta(z_7+z_8+z_9+z_{10}+z_{11}+z_{12})$,
F 2: $s_6=(1/\sqrt{12})\Delta(z_{13}+z_{14}+z_{15}+z_{16}+z_{17}+z_{18}+z_{19}+z_{20}+z_{21}+z_{22}+z_{23}+z_{24})$,
F 2: $s_7=(1/\sqrt{12})\Delta\{(x_{13}+(-x_{14}+\sqrt{3}y_{14})/2+(-x_{15}-\sqrt{3}y_{15})/2-x_{16}-(-x_{17}+\sqrt{3}y_{17})/2-(-x_{18}-\sqrt{3}y_{18})/2+x_{19}+(-x_{20}+\sqrt{3}y_{20})/2+(-x_{21}-\sqrt{3}y_{21})/2-x_{22}-(-x_{23}+\sqrt{3}y_{23})/2-(-x_{24}-\sqrt{3}y_{24})/2),\}$

(E_{1u})

Ni 1: $s_1=(1/\sqrt{2})\Delta(x_1+x_2)$,
s_2=the same for y_i,
Ni 2: $s_3=(1/\sqrt{4})\Delta(x_3+x_4+x_5+x_6)$,
s_4=the same for y_i,
Rb 1: $s_5=(1/\sqrt{2})\Delta(x_{25}+x_{26})$,
s_6=the same for y_i,
Rb 2: $s_7=(1/\sqrt{4})\Delta(x_{27}+x_{28}+x_{29}+x_{30})$,
s_8=the same for y_i,
F 1: $s_9=(1/\sqrt{6})\Delta(x_7+x_8+x_9+x_{10}+x_{11}+x_{12})$,
s_{10}=the same for y_i,
F 1: $s_{11}=(1/\sqrt{6})\Delta\{(x_7+(-x_8-\sqrt{3}y_8)/2+(-x_9+\sqrt{3}y_9)/2+x_{10}+(-x_{11}-\sqrt{3}y_{11})/2+(-x_{12}+\sqrt{3}y_{12})/2)\}$,
F 1: $s_{12}=(1/\sqrt{6})\Delta\{(y_7+(\sqrt{3}x_8-y_8)/2+(-\sqrt{3}x_9-y_9)/2+y_{10}+(\sqrt{3}x_{11}-y_{11})/2+(-\sqrt{3}x_{12}-y_{12})/2)\}$,
F 2: $s_{13}=(1/\sqrt{12})(x_{13}+x_{14}+x_{15}+x_{16}+x_{17}+x_{18}+x_{19}+x_{20}+x_{21}+x_{22}+x_{23}+x_{24})$,
s_{14}=the same for y_i,
F 2: $s_{15}=(1/\sqrt{12})\Delta\{(x_{13}+(-x_{14}-\sqrt{3}y_{14})/2+(-x_{15}+\sqrt{3}y_{15})/2+x_{16}+(-x_{17}-\sqrt{3}y_{17})/2+(-x_{18}+\sqrt{3}y_{18})/2+x_{19}+(-x_{20}-\sqrt{3}y_{20})/2+(-x_{21}+\sqrt{3}y_{21})/2+x_{22}+(-x_{23}-\sqrt{3}y_{23})/2+(-x_{24}+\sqrt{3}y_{24})/2)\}$,
F 2: $s_{16}=(1/\sqrt{12})\Delta\{(y_{13}+(\sqrt{3}x_{14}-y_{14})/2+(-\sqrt{3}x_{15}-y_{15})/2+y_{16}+(\sqrt{3}x_{17}-y_{17})/2+(-\sqrt{3}x_{18}-y_{18})/2+y_{19}+(\sqrt{3}x_{20}-y_{20})/2+(-\sqrt{3}x_{21}-y_{21})/2+y_{22}+(\sqrt{3}x_{23}-y_{23})/2+(-\sqrt{3}x_{24}-y_{24})/2)\}$,
F 2: $s_{17}=(1/\sqrt{24})\Delta\{(2z_{13}-z_{14}-z_{15}-2z_{16}+z_{17}+z_{18}+2z_{19}-z_{20}-z_{21}-2z_{22}+z_{23}+z_{24})\}$,
$s_{18}=(1/\sqrt{8})\Delta\{(z_{14}-z_{15}-z_{17}+z_{18}+z_{20}-z_{21}-z_{23}+z_{24})\}$.

2) $CsNiF_3$ 2L: If ions are appropriately indexed, the Cartesian symmetry coordinates has the same expressions as those of $RbNiF_3$ 6L. Then in (A_{2u}), only s_1, s_3, and s_5 in $RbNiF_3$ 6L appear, and in (E_{1u}), only s_1, s_2, s_5, s_6, s_9, s_{10}, s_{11}, and s_{12} in $RbNiF_3$ 6L appear.

3) $CsNiF_3$ 9L: Ions with the Cartesian coordinates given in the parenthesis are indexed as follows:

1 Ni 1; $(0, 0, 0)$
2 Ni 2; $(0, 0, w_1c)$
3 Ni 2; $(0, 0, -w_1c)$
4 F 1; $(-a/2\sqrt{3}, 0, c/6)$
5 F 1; $(a/4\sqrt{3}, -a/4, c/6)$
6 F 1; $(a/4\sqrt{3}, a/4, c/6)$
7 F 2; $(\sqrt{3}u_2a, 0, w_2c)$
8 F 2; $((-\sqrt{3}/2)u_2a, (3/2)u_2a, w_2c)$
9 F 2; $((-\sqrt{3}/2)u_2a, (-3/2)u_2a, w_2c)$
10 F 2; $(-\sqrt{3}u_2a, 0, -w_2c)$
11 F 2; $((\sqrt{3}/2)u_2a, (-3/2)u_2a, -w_2c)$
12 F 2; $((\sqrt{3}/2)u_2a, (3/2)u_2a, -w_2c)$
13 Cs 1; $(\sqrt{3}a, 0, c/6)$
14 Cs 2; $(0, 0, w_3c)$
15 Cs 2; $(0, 0, -w_3c)$,

where u_i's and w_i's are parameter values (Table 1). Then the symmetry coordinates of A_{2u} and E_u species are as follows.

(A_{2u})

Ni 1: $s_1=\Delta z_1$,
Ni 2: $s_2=(1/\sqrt{2})\Delta(z_2+z_3)$,
Cs 1: $s_3=\Delta z_{13}$,
Cs 2: $s_4=(1/\sqrt{2})\Delta(z_{14}+z_{15})$,
F 1: $s_5=(1/\sqrt{3})\Delta(z_4+z_5+z_6)$,
F 1: $s_6=(1/\sqrt{3})\Delta\{(x_4+(-x_5+\sqrt{3}y_5)/2+(-x_6-\sqrt{3}y_6)/2)\}$,
F 2: $s_7=(1/\sqrt{6})\Delta(z_7+z_8+z_9+z_{10}+z_{11}+z_{12})$,
F 2: $s_8=(1/\sqrt{6})\Delta(x_7+(-x_8+\sqrt{3}y_8)/2+(-x_9-\sqrt{3}y_9)/2+x_{10}+(-x_{11}+\sqrt{3}y_{11})/2+(-x_{12}-\sqrt{3}y_{12})/2)$,

(E_u)

Ni 1: $s_1=\Delta x_1$, s_2=the same for y_i,

Ni 2: $s_3=(1/\sqrt{2})\Delta(x_2+x_3)$, $s_4=$the same for y_i,
Cs 1: $s_5=\Delta x_{13}$, $s_6=$the same for y_i,
Cs 2: $s_7=(1/\sqrt{2})\Delta(x_{14}+x_{15})$, $s_8=$the same for y_i,
F 1: $s_9=(1/\sqrt{3})\Delta(x_4+x_5+x_6)$,
$s_{10}=$the same for y_i,
F 1: $s_{11}=(1/\sqrt{3})\Delta\{(x_4+(-x_5-\sqrt{3}y_5)/2+(-x_6+\sqrt{3}y_6)/2)\}$,
F 1: $s_{12}=(1/\sqrt{3})\Delta\{(y_4+(\sqrt{3}x_5-y_5)/2+(-\sqrt{3}x_6-y_6)/2)\}$,
F 1: $s_{13}=(1/\sqrt{6})\Delta(2z_4-z_5-z_6)$,
F 1: $s_{14}=(1/\sqrt{2})\Delta(z_5-z_6)$,
F 2: $s_{15}=(1/\sqrt{6})\Delta(x_7+x_8+x_9+x_{10}+x_{11}+x_{12})$
$s_{16}=$the same for y_i,
F 2: $s_{17}=(1/\sqrt{6})\Delta\{(x_7+(-x_8-\sqrt{3}y_8)/2+(-x_9+\sqrt{3}y_9)/2+x_{10}+(-x_{11}-\sqrt{3}y_{11})/2+(-x_{12}+\sqrt{3}y_{12})/2)\}$,
F 2: $s_{18}=(1/\sqrt{6})\Delta\{(y_7+(\sqrt{3}x_8-y_8)/2+(-\sqrt{3}x_9-y_9)/2+y_{10}+(\sqrt{3}x_{11}-y_{11})/2+(-\sqrt{3}x_{12}-y_{12})/2)\}$,
F 2: $s_{19}=(1/\sqrt{12})\Delta(2z_7-z_8-z_9+2z_{10}-z_{11}-z_{12})$,
F 2: $s_{20}=(1/\sqrt{4})\Delta(z_8-z_9+z_{11}-z_{12})$.